# Photoresist-Derived Carbon for Microelectromechanical Systems and Electrochemical Applications

**Article** *in* Journal of The Electrochemical Society · January 2000

DOI: 10.1149/1.1393188

CITATIONS
264

READS
217

**4 authors**, including:

Marc J. Madou
University of California, Irvine
**488** PUBLICATIONS **13,260** CITATIONS

SEE PROFILE

*Journal of The Electrochemical Society*, **147** (1) 277-282 (2000)
S0013-4651(99)02-055-8 CCC: $7.00 


# Photoresist-Derived Carbon for Microelectromechanical Systems and Electrochemical Applications

**Srikanth Ranganathan,[a] Richard McCreery,[a,*] Sree Mouli Majji,[b] and Marc Madou[a,b,z]**

[a]*Department of Chemistry and* [b]*Department of Materials Science and Engineering, The Ohio State University, Columbus, Ohio 43210, USA*

Photopatterned resists pyrolyzed at different temperatures and different ambient atmospheres can be used as a carbonaceous material for microelectromechanical systems. Carbon films were prepared by pyrolysis of photoresists at temperatures ranging from 600 to 1100°C. The carbon films were characterized by several analytical techniques, viz., profilometry, thermogravimetric analysis, four-point probe measurements, scanning electron microscopy, transmission electron microscopy, atomic force microscopy, X-ray photoelectron spectroscopy (XPS), and Raman spectroscopy. In addition, cyclic voltammetry was performed on the carbon film electrodes, and the carbon films were compared to glassy carbon (GC) for their electrochemical behavior. Electron-transfer rate constants for the benchmark $Fe(CN)_6^{3-/4-}$ and $Ru(NH_3)_6^{3+/2+}$ redox systems increased with increasing heat-treatment temperature, and approached those observed on GC following treatment at 1100°C. The pyrolyzed films have low capacitance and background current, approximately one-fourth of that observed on GC. The oxygen/carbon atomic ratio determined from XPS was low (~1% for 1100°C pretreatment), and increased more slowly upon exposure to air than that for GC treated under identical conditions. Pyrolysis of photoresist films permits photolithographic fabrication of carbon electrode devices, and also appears to yield a carbon film with a smooth surface and unusual surface chemistry.


Manuscript submitted February 12, 1999; revised manuscript received July 28, 1999.

Conventionally, microelectromechanical systems (MEMS) have been based mostly on silicon.[1] In this paper, we describe work carried out to evaluate carbon films produced by the pyrolysis of photoresists for use in MEMS and as electrode materials.[2] These carbon electrodes have potential applications in batteries, electrochemical sensors, and capacitors and in electrochemically based MEMS devices. The advantage of using photoresists as the starting material is that the photoresists can be patterned by photolithography techniques, and hence complex-shaped electrodes can be produced. Photoresists are used extensively in the integrated circuits industry and are very reproducible in their behavior, and hence the carbon films produced by pyrolyzing these photoresists constitute a potentially reliable carbon source.

Carbon materials have been used extensively for electroanalytical chemistry, electrosynthetic chemistry, and energy conversion; several reviews are available.[3-7] Directly relevant to the current report are examinations of carbon films made from pyrolysis of gases,[8-13] pyrolysis of sublimed organic films,[14,15] sputtered carbon films,[16] pyrolyzed photoresists,[2,17,18] and patterned organic films of polyacrylonitrile[19,20] and poly(furfuryl alcohol) resin.[21-23] The electrochemical properties of these carbon materials vary with fabrication temperature and pretreatment procedures, but most show quasi-reversible electron-transfer behavior, with rate constants for $Fe(CN)_6^{3-/4-}$ in the range of $10^{-3}$ to $10^{-2}$ cm/s.

This report deals with the preparation, characterization, and electrochemical behavior of carbon films made from a positive photoresist material. The carbon films exhibit fast electron transfer to $Fe(CN)_6^{3-/4-}$ and $Ru(NH_3)_6^{3+/2+}$, but also have unusual properties with respect to surface oxidation. Of emphasis in this study is the nature of the carbon surface and its suitability for electrochemical applications.

## Experimental

*Carbon film preparation.*—A positive photoresist, AZ4330 (Hoechst Celanese, Somerville, NJ), was used to form conductive carbon films. The carbon films obtained from the AZ4330 photoresist are referred to as the AZ film. Silicon wafers (2 in. CZ, n-type, <1-0-0> oriented, 13-17 mil, 1-20 Ω) were dipped in a dilute hydrofluoric acid solution before being spin-coated with a thin layer of the photoresist. The photoresist was applied manually on a silicon wafer spinning at 6000 rpm for 30 s in a spin coater. Multiple applications of the photoresist were performed to produce a final thickness of about 5-6 μm before pyrolysis. The photoresist films were carbonized by heating in different ambient gases at 600, 700, 800, 900, 1000, or 1100°C. The pyrolysis atmospheres included: $10^{-5}$ Torr vacuum maintained with a turbo pump; $10^{-7}$ Torr vacuum from a turbo pump; 99.999% $N_2$ at 1 atm, and forming gas (95% $N_2$, 5% $H_2$) at 1 atm. $N_2$ and forming gas were flowing at approximately 15 standard cubic centimeters per minute (sccm) during and after pyrolysis. The pyrolyzed samples were cooled to room temperature in the pyrolysis atmosphere before exposure to air. In all cases, samples were heated at 20°C/min, and held at the maximum temperature for 60 min before cooling.

*Carbon film characterization.*—The thickness of the carbon films before and after pyrolysis was determined using a profilometer. A small groove was made in the film so that the silicon beneath was exposed, and a surface profile was taken by moving the profiler stylus across the groove. The thickness of the resist film was determined from the difference in height between the photoresist and uncoated silicon. Three such profiles were taken on each film, and the average value was calculated. For thermogravimetric analysis (TGA), a small amount of the photoresist was heated in an oven at 100°C for about 3 h to dry the resist by evaporating the solvent. A four-point probe was used to calculate the sheet resistance of the carbon films. Scanning electron microscopy (SEM) was employed to observe the surface porosity of the films, and transmission electron microscopy (TEM) was used for microstructure analysis. Atomic force microscopy (AFM) was performed to study the film surface morphology. Raman spectroscopy (514.5 nm, Dilor X-Y spectrometer for microscopy, Kaiser Holospec for conventional Raman) was used on the films to investigate the presence of any characteristic graphite peaks. X-ray photoelectron spectroscopy (XPS) with a VG Escalab spectrometer was performed to determine the oxygen coverage on the films, based on $O_{1s}$ and $C_{1s}$ peak area ratios, corrected for instrumental sensitivity. The O/C atomic ratios of the vacuum pyrolyzed samples were determined immediately after pyrolysis, whereas the O/C atomic ratios of the films pyrolyzed in forming gas were determined after 3-4 days of exposure to laboratory air. Cyclic voltammetry was performed with a Bioanalytical Systems BAS 100 potentiostat on electrodes fashioned from the pyrolyzed photoresist. Both sides of the pyrolyzed photoresist sample were exposed to the electrolyte (with carbon film on one side and insulating $SiO_2$ on the

* Electrochemical Society Active Member.
z E-mail: madou.1@osu.edu

S0013-4651(99)02-055-8 CCC: $7.00 

other), to reduce the possibility of film damage by a cell or O-ring. Approximately 0.5 $cm^2$ of pyrolyzed photoresist and an equal area of unmodified silicon were exposed to solution in typical voltammetry experiments. Background voltammograms with an uncoated silicon sample and a silicon sample coated with unpyrolyzed photoresist showed no voltammetric features and low background current. To determine sheet resistance, a probe head containing four closely placed tungsten probe tips was placed on the surface of the resist film. A known value of current ($I$) was passed between the two outer probes using a current source, and the potential ($V$) was measured between the two inner probes. The sheet resistance was calculated as

$$R_S = (V/I)CF$$

where $CF$ is a sheet resistance correction factor that depends on the sample dimensions and the probe tip spacing. To fabricate patterned electrodes, exposure of the photoresist was performed with a Cobilt mask aligner, and AZ400K developer (Hoechst Celanese, Somerville, NJ) was used for the development of the image. The developed structure was pyrolyzed in a nitrogen atmosphere at 900°C.

## Results

*Film shrinkage and weight loss.*—Film thickness after pyrolysis was typically 1-2 μm. The percent shrinkage of the resist films is reported in Table I. The shrinkage occurred almost totally in thickness; changes in lateral dimensions were minor. The shrinkage depended on curing atmosphere, with the high vacuum ($10^{-7}$ Torr) producing the lowest, and nitrogen generally producing the highest shrinkage. These differences are presumably due to trace oxygen in the curing atmosphere. Lyons *et al.*[17] showed that the difference in shrinkage for a different photoresist between pure $H_2$ and pure $N_2$ atmospheres was about 10%, so a reaction between carbon and $H_2$ does not appear to be a major factor in determining shrinkage.

*TGA.*—A TGA plot of weight loss *vs.* time for a 11.8 mg sample of dried AZ4330 photoresist heated in nitrogen is shown in Fig. 1. The TGA was performed in the temperature range of 20 to 1200°C, at a heating rate of 50°C/min from 20 to 400°C and at a rate of 20°C/min from 400 to 1200°C. Starting with dried AZ4330 resist, there are significant weight losses of ~11% between 150 and 250°C, another 49% between 250 and 500°C, and a more gradual loss of an additional 9% between 500 and 1200°C. The final weight at 1200°C is 31% of the initial dry weight for the case of a nitrogen atmosphere. This compares to a film thickness of 20% of the original for 1000°C in nitrogen, implying that the pyrolyzed film is denser than the original photoresist. Based on pyrolysis of organic polymers,[24] the early weight loss coincides with the loss of $H_2O$, CO, and $CO_2$, while higher temperature weight loss accompanies aromatization. Combined with the film shrinkage, the weight loss corresponds to an increase in density of approximately 55% for the case of a nitrogen atmosphere.

*Sheet resistance.*—The values of sheet resistance for the resist films pyrolyzed at various temperatures in forming gas are given in Table II. The AZ carbon films at 600°C yielded unstable resistance values, and the number reported is questionable. The carbon film obtained at 700°C still shows very high resistance, but stable measurements could be made. The resistance decreased dramatically for the carbon films produced at 800°C and above.

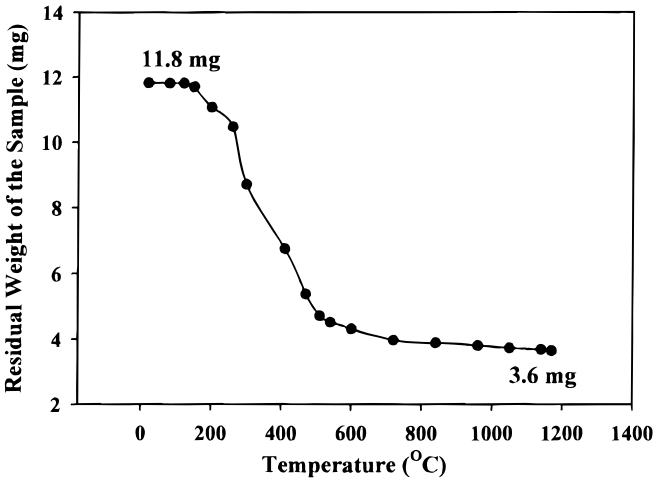


**Figure 1.** Thermogravimetric analysis of AZ4330 photoresist in nitrogen atmosphere.

The lowest value observed for sheet resistance was 51.2 Ω/□ for the 1100°C heat-treatment in forming gas. For a film thickness of 1.0 μm, this corresponds to a resistivity of $5.1 \times 10^{-3}$ Ω cm for the carbon film. For comparison, Tokai glassy carbon (GC) has a resistivity of (4.5-5.0) $\times 10^{-3}$ Ω cm for 1000°C heat-treatment and (4.0-4.5) $\times 10^{-3}$ Ω cm for 2000°C heat-treatment.[3] As is the case with several other carbon materials, the resistivity may be varied over a wide range depending on heat-treatment temperature, ranging from that of a semiconductor to that of a conductor over the 600 to 1100°C range.

*Microscopy.*—The SEM images of the AZ carbon films produced in different furnace atmospheres are featureless, with no evidence for porosity at several high magnifications. High resolution TEM of a small chip of pyrolyzed photoresist supported on a gold grid indicated the presence of areas of graphite-like structures in an amorphous carbon film. One such example of the graphite-like crystal planes observed in the amorphous carbon matrix is shown in Fig. 2. The lattice image for the (002) plane was evident in the carbon films, even for those obtained by heat-treatment at 600°C. The (002) diffraction ring was observed by selected-area electron diffraction, and it is more prominent in the carbon films obtained by pyrolysis at 1000 and 1100°C. The extent of graphite microcrystallites apparent in Fig. 2 appears to be greater than that reported for similar materials by Kinoshita *et al.*[2] for currently unknown reasons. AFM images of several 1 × 1 μm regions of the pyrolyzed film were featureless and showed no evidence of porosity. The root mean square (rms) roughness of the pyrolyzed surface judged from AFM was approximately 1 nm. Previous scanning tunnel microscope (STM) results on GC report an rms roughness in the range of 4.1 to 4.5 nm for polished, heat-treated, and laser-activated (25 $mW/cm^2$) surfaces.[25]

**Table I. Carbon film shrinkage in various furnace atmospheres.**

| Temperature of pyrolysis (°C) | % Reduction in film thickness in Vacuum ($10^{-7}$ Torr) | Vacuum ($10^{-5}$ Torr) | Forming gas | Nitrogen |
|---|---|---|---|---|
| 600 | 50.34 | 50.73 | 56.06 | 61.64 |
| 700 | 51.22 | 57.01 | 57.05 | 73.95 |
| 800 | 57.77 | 60.82 | 58.07 | 78.51 |
| 900 | 61.51 | 66.33 | 73.90 | 86.57 |
| 1000 | 65.21 | 70.98 | 81.60 | 80.51 |
| 1100 | — | — | 83.59 | — |

**Table II. Sheet resistance of the AZ carbon films pyrolyzed at various temperatures.**

| Temperature of pyrolysis (°C) | Sheet resistance (Ω/□) |
|---|---|
| 600 | 146.4 |
| 700 | 845.8 |
| 800 | 244.8 |
| 900 | 94.3 |
| 1000 | 57.1 |
| 1100 | 51.2 |

S0013-4651(99)02-055-8 CCC: $7.00 

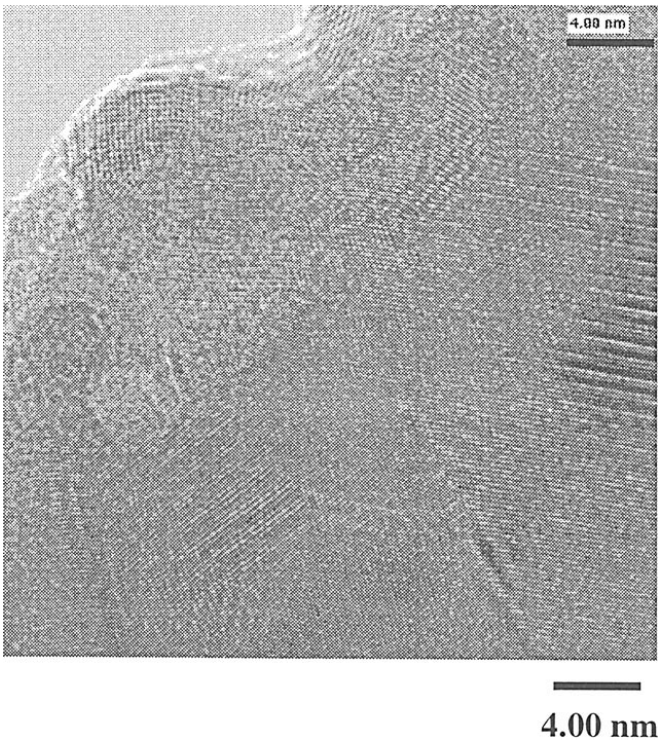


**Figure 2.** High resolution TEM image taken on a carbon film produced by the pyrolysis of AZ4330 photoresist in forming gas atmosphere at 900°C.

*Raman spectroscopy.*—Raman spectra of the AZ photoresist were acquired after pyrolyzing under various conditions, in order to assess the development of the characteristic $sp^2$ carbon bands at ~1360 and ~1600 $cm^{-1}$. The "D" (~1360 $cm^{-1}$) and "$E_{2g}$" (~1582 $cm^{-1}$) bands have been studied extensively, and their peak area ratio ($D/E_{2g}$ ratio) has been correlated with disorder of the $sp^2$ carbon matrix.[26,27] A larger $D/E_{2g}$ ratio correlates with smaller graphite crystallite size ($L_a$), and indicates greater disorder. The unpyrolyzed photoresist itself was strongly fluorescent, and a Raman spectrum was not obtainable. Spectra acquired after heat-treatment in forming gas are shown in Fig. 3, with GC for comparison. Baseline resolution of the D and $E_{2g}$ bands was not observed for the pyrolyzed film. However, higher treatment temperature does cause band narrowing, indicating less disorder following higher temperature curing. This behavior is qualitatively similar to other types of pyrolyzed carbon, including carbon fibers. The apparent feature at approximately 1180 $cm^{-1}$ is

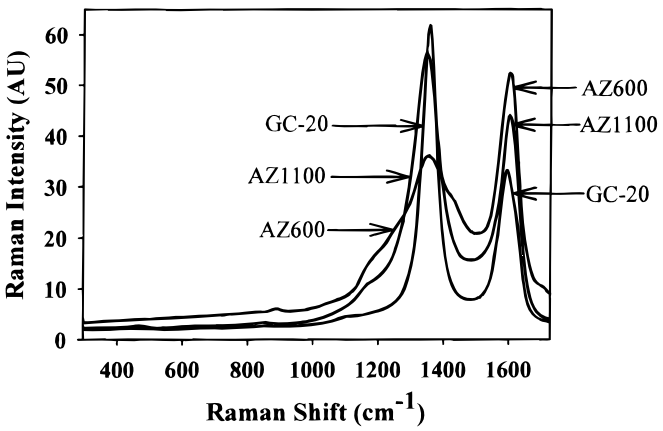


**Figure 3.** Raman spectra of the AZ carbon films compared with glassy carbon. AZ1100: AZ carbon films pyrolyzed at 1100°C, AZ600: AZ carbon films pyrolyzed at 600°C, and GC-20: glassy carbon heat-treated at 2000°C.

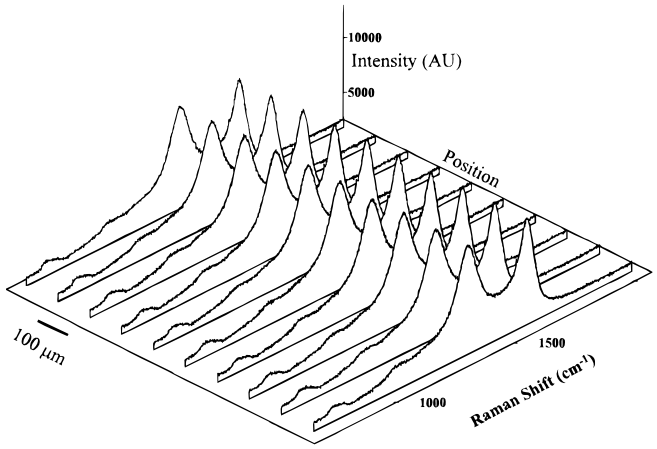


**Figure 4.** Raman profile of an AZ carbon film pyrolyzed at 1100°C. Ten Raman spectra taken along a 900 μm line with a spot size of ~10 μm are shown. The sample was not refocused between acquisitions.

reproducible but currently unidentified. The furnace atmosphere did not have a large effect on the Raman spectra, although the $D/E_{2g}$ band area ratio was slightly higher for vacuum treatment compared to forming gas, at all temperatures studied. Figure 4 shows a series of 10 microscopic Raman spectra acquired along a 900 μm line with a spot size of ~10 μm (10 times microscope objective). The constant $D/E_{2g}$ ratio along the 900 μm line indicates a uniform microstructure of the pyrolyzed film on a scale of the laser spot size (~10 μm). Equally constant spectra and $D/E_{2g}$ ratios were obtained along a 150 μm line using an ~1 μm spot size (100 times objective). Constant intensities imply a smooth surface, since the microscope focus was maintained along the 900 μm line. In fact, the smooth, featureless surface of the pyrolyzed photoresist made it difficult to focus both the optical and SEM probes.

*XPS.*—The unpyrolyzed resist showed an atomic O/C ratio of 22%. The observed O/C atomic ratios following curing at several temperatures in both vacuum and forming gas are listed in Table III. The vacuum apparatus employed for curing did not permit pyrolysis temperatures above 1000°C. The atmosphere did not have a large effect on the O/C atomic ratios until the higher temperatures were reached (1000-1100° C). The very low O/C ratio observed following pyrolysis at 1100°C (1.2%) increased slowly with air exposure. Heat-treated GC with comparably low initial O/C showed a much more rapid increase in O/C with air exposure, reaching ~6% in 24 h. Although contamination by hydrocarbons from lab air may affect the observed O/C ratio, it is clear that the pyrolyzed films are oxidized much more slowly than GC. When studied as a function of treatment temperature, the O/C ratio for pyrolyzed photoresist decreased greatly from the unpyrolyzed value, and decreased slowly between 600 and 1000°C. Forming gas at 1100°C yielded a very low O/C atomic

**Table III. Atomic O/C ratios of the pyrolyzed AZ carbon films, from XPS.**

| Pyrolysis temperature (°C) | Forming gas[a] (%) | Vacuum[b] ($10^{-5}$ Torr) | Vacuum[b] ($10^{-7}$ Torr) |
|---|---|---|---|
| 600 | 6.7 | 6.4 | 5.4 |
| 700 | 6.4 | 5.6 | 4.1 |
| 800 | 9.3 | 4.9 | 5.2 |
| 900 | 5.0 | 4.9 | 4.6 |
| 1000 | 4.7 | 5.5 | 3.5 |
| 1100 | 1.2 | — | — |

[a] XPS spectra obtained after 3-4 days of air exposure.
[b] XPS spectra obtained immediately after pyrolysis.

S0013-4651(99)02-055-8 CCC: $7.00 

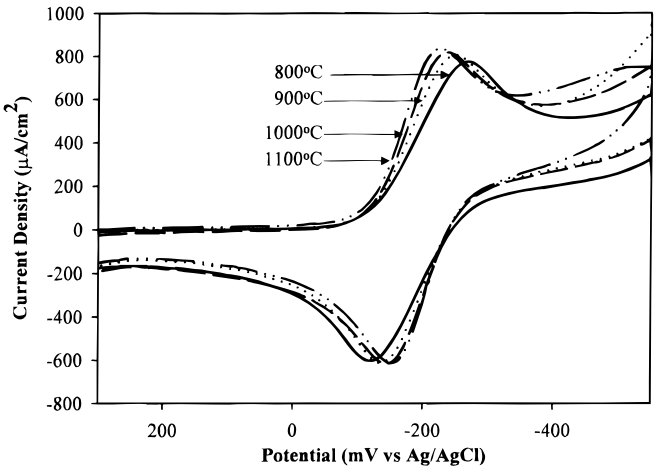


**Figure 5.** Cyclic voltammograms of 1 mm $[Ru(NH_3)_6]^{3+/2+}$ in 1 M KCl on AZ carbon films pyrolyzed in forming gas atmosphere. The scan rate used is 200 mV/s.

ratio (1.2%), even after the surface was exposed to air for 4 days. Improving the vacuum during curing reduced the O/C atomic ratio, presumably due to the lower oxygen level in the curing atmosphere.

*Electrochemical measurements.*—$Ru(NH_3)_6^{3+/2+}$ has been shown to be relatively insensitive to surface films and functional groups on carbon,[6,28] and was examined as a simple outer sphere redox system. Electron-transfer rate constants for $Ru(NH_3)_6^{3+/2+}$ on clean GC are comparable to those on metals, and are not seriously affected by surface monolayers or oxides.[27] In addition, $Fe(CN)_6^{3-/4-}$ was examined due to extensive comparative data in the literature,[6,7,29] including previous measurements on pyrolyzed photoresist.[2] Figure 5 shows cyclic voltammograms of $Ru(NH_3)_6^{3+/2+}$ obtained on the surface of carbon films pyrolyzed at several temperatures. Table IV lists observed $\Delta E_p$ (the difference in the peak potentials) values for 1 mM and 0.1 mM $Ru(NH_3)_6^{3+/2+}$ in 1 M KCl, for electrodes formed in both vacuum and forming gas atmospheres. For 800 and 900°C treatment, $\Delta E_p$ s for 1 mM $Ru(NH_3)_6^{3+/2+}$ were larger than for 0.1 mM, implying a significant contribution from the *iR* drop in the electrode itself. This table also lists $\Delta E_p$ values for 1 mM and 0.1 mM $Fe(CN)_6^{3-/4-}$ in 0.1 M $H_2SO_4$. $\Delta E_p$ decreases for higher treatment temperature, at least partly due to the lower resistance. The effect of film resistance on the observed $\Delta E_p$ was examined in more detail by two different approaches. First, the expected resistance for the film was calculated from the measured sheet resistance at various curing temperatures (Table II) and the geometric dimensions of the film. The results are shown in Table V. Second, the resistance was estimated by adjusting the cell resistance as an input to a simulation program (Digisim, Bioanalytical Systems, West Lafayette, IN) until the simulated voltammograms matched the experimental result. As shown in Table V, the two determinations of resistance agree very well. Also listed in Table V is the corrected $\Delta E_p$ obtained by subtracting the *iR* error calculated from the sheet resistance and peak current. The corrected $\Delta E_p$ decreases with curing temperature, indicating an increase in electron-transfer rate with curing temperature. At 1100°C, the rate constant ($k^0$) for $Ru(NH_3)_6^{3+/2+}$ determined from the corrected $\Delta E_p$ is 0.055 cm/s. This rate constant compares favorably with those observed for clean GC (0.1-0.25 cm/s).[7,26] Treatment of polished GC in the 1000°C forming gas atmosphere under the same conditions as pyrolyzed photoresist yielded a rate constant for both 1.0 and 0.1 mM $Ru(NH_3)_6^{3+/2+}$ of 0.04 cm/s. The $Fe(CN)_6^{3-/4-}$ redox couple in 1 M KCl also exhibited ohmic potential error on pyrolyzed films, and exhibited behavior similar to that of $Ru(NH_3)_6^{3+/2+}$. (See Table VI) For a 1000°C film, the uncorrected $k^0$ for $Fe(CN)_6^{3-/4-}$ was 0.015 cm/s, and was 0.042 cm/s after correction of $\Delta E_p$ for film resistance.

The voltammetric background current in 1 M KCl was lower for pyrolyzed photoresist than for GC, following the same pretreatment. The apparent capacitance determined from the voltammetric background current for a film treated at 1000°C in forming gas was 8 $\mu F/cm^2$, while that for GC after the same heat-treatment was ~35 $\mu F/cm^2$. These values compare with previously reported values of 33 ± 6 $\mu F/cm^2$ for polished GC, 75 ± 16 $\mu F/cm^2$ for fractured GC, and 34 $\mu F/cm^2$ for laser-activated GC.[25] Cleaning with isopropyl alcohol containing activated carbon increased the pyrolyzed photoresist capacitance to 9.2 $\mu F/cm^2$, while the same treatment increased the capacitance of a polished GC electrode from 38 to 66 $\mu F/cm^2$. [30]

*Fabrication of carbon microstructures.*—Photolithography was used to fabricate an interdigitated electrode on the basis of AZ4330 photoresist, using standard techniques.[31] Figure 6 shows a SEM image of a section of the interdigitated electrode after pyrolysis. The darker regions in the image correspond to the carbon; the lighter regions correspond to the silicon substrate. The carbon stripes are ~950 μm wide and 2 μm thick, while the gap separating the interdigitated fingers is ~88 μm wide. On pyrolysis, a shrinkage of ~71% of the photoresist film was observed in thickness, but no lateral shrinkage or distortion of the structure was observed.

## Discussion

"Pyrolyzed carbon film" is a general term applied to carbon films made under a variety of conditions and having a range of properties. To distinguish the materials in this article and point out their utility for microfabrication, we refer to them as pyrolyzed photoresist films (PPF). The primary emphasis of this discussion is their electrochemical properties, which are compared to those of several similar materials in Table VII. Not all of the investigations listed used identical conditions, but several observations deserve special note. First, the resistivity of PPF is comparable to that of GC, and at the low end of the range observed for other pyrolysis procedures. Second, the rate constant for $Fe(CN)_6^{3-/4-}$ is at least as high as that for other thin carbon

**Table IV. Variation of $\Delta E_p$ of the AZ carbon films (pyrolyzed in forming gas and vacuum) with the temperature of pyrolysis.**

| Curing temperature (°C) | 1 mM $[Ru(NH_3)_6]^{+3/+2}$ in 1 M KCl Scan rate: = 200 mV/s | | 1 mM $Fe(CN)_6^{3-/4-}$ in 0.1 M $H_2SO_4$ Scan rate: = 200 mV/s | 0.1 mM $[Ru(NH_3)_6]^{+3/+2}$ in 1 M KCl Scan rate: = 200 mV/s | | 0.1 mM $Fe(CN)_6^{3-/4-}$ in 0.1 M $H_2SO_4$ Scan rate: = 200 mV/s |
|---|---|---|---|---|---|---|
| | $\Delta E_p$ (Forming gas, mV) | $\Delta E_p$ (Vacuum, mV) | $\Delta E_p$ (Forming gas, mV) | $\Delta E_p$ (Forming gas, mV) | $\Delta E_p$ (Vacuum, mV) | $\Delta E_p$ (Forming gas, mV) |
| 600 | — | — | — | — | — | — |
| 700 | — | 87 | — | — | 158 | 339 |
| 800 | 146 | 92 | 142 | 88 | 100 | 77 |
| 900 | 109 | 93 | 101 | 72 | 90 | 69 |
| 1000 | 88 | 98 | 90 | 70 | 84 | 80 |
| 1100 | 70 | — | 84 | 70 | — | 63 |
| Polished GC | 60 | 60 | 65 | 60 | 60 | 54 |

S0013-4651(99)02-055-8 CCC: $7.00 

**Table V. Correction for $\Delta E_p$ due to *iR* (AZ carbon films pyrolyzed in forming gas).**

(a) Redox system: 1 mM $[Ru(NH_3)_6]^{3+/2+}$, scan rate: 200 mV/s

| Temperature (°C) | $\Delta E_p$ (mV) | *R* from fit (Ω) | *R* from sheet resistance (Ω) | Corrected $\Delta E_p$ using sheet resistance (mV) |
|---|---|---|---|---|
| 800 | 146 | 209 | 190 | 84 |
| 900 | 109 | 90 | 82 | 74 |
| 1000 | 88 | 60 | 65 | 67 |
| 1100 | 70 | 29 | 38 | 63 |

(b) Redox System: 0.1 mM $[Ru(NH_3)_6]^{3+/2+}$, scan rate: 200 mV/s

| Temperature (°C) | $\Delta E_p$ (mV) | *R* from sheet resistance (Ω) | Corrected $\Delta E_p$ using sheet resistance (mV) |
|---|---|---|---|
| 800 | 88 | 190 | 82 |
| 900 | 72 | 82 | 67 |
| 1000 | 70 | 65 | 67 |
| 1100 | 70 | 38 | 69 |

**Table VI. $\Delta E_p$ for 1 mM $Fe(CN)_6^{3-/4-}$ in 1 M KCl (AZ films pyrolyzed in forming gas).**

| Curing Temperature (°C) | Scan rate: = 200 mV/s $\Delta E_p$ (mV) | Scan rate: = 2 V/s $\Delta E_p$ (mV) | Scan rate: = 20 V/s $\Delta E_p$ (mV) |
|---|---|---|---|
| 600 | — | — | — |
| 700 | — | — | — |
| 800 | 277 | 471 | — |
| 900 | 200 | 365 | >600 |
| 1000 | 152 | 304 | >600 |
| 1100 | 80 | 125 | 263 |
| Polished GC | 65 | 73 | 96 |

films, and within an order of magnitude of GC itself. $Ru(NH_3)_3^{3+/2+}$ rate constants were not reported for most materials listed in Table VII, but the PPF value of ~0.05 cm/s compares favorably with 0.04 for similarly prepared GC. The increase in $k^0$ values with pyrolysis temperature is likely to be due to the decrease in resistance and the gradual filling in of the bandgap as graphitization occurs. For the current

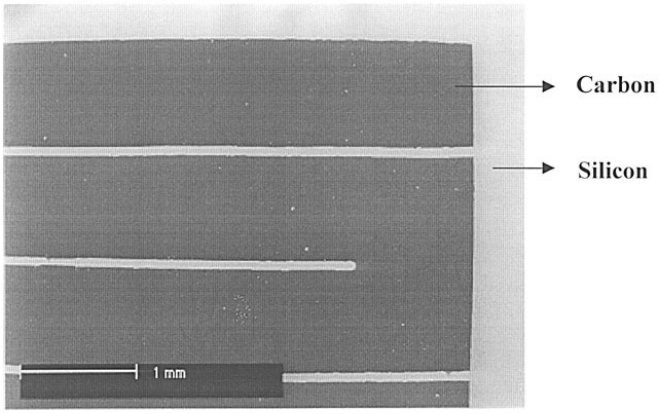


**Figure 6.** SEM image of a section of the photolithographically patterned carbon electrode after pyrolysis at 900°C in forming gas.. The image shows darker regions of carbon separated by lighter regions of silicon.

conditions, the kinetics of $Ru(NH_3)_3^{3+/2+}$ were indistinguishable on 1000° PPF or on GC treated in 1000° forming gas. At least by the criteria considered in Table VII, PPF has good properties as an electrochemical sensor, with the added feature of photolithographic capability. Redox systems vary significantly in their sensitivity to the state of the carbon surface,[28] and the PPF surface may behave quite differently from GC for systems other than $Ru(NH_3)_3^{3+/2+}$ and $Fe(CN)_6^{3-/4-}$.

The low capacitance of PPF observed by voltammetry (8 μF/cm$^2$) is important for possible analytical applications, and represents contributions both from double-layer capacitance and surface redox reactions. The low O/C ratio of PPF should reduce the density of redox active surface groups such as quinones, thus reducing the faradaic contribution to observed capacitance. The unusually low value of 8 μF/cm$^2$ for PPF is matched only by the sputtered films of Schlesinger *et al.*,[16] which had a capacitance of 7.5 μF/cm$^2$. The low value for sputtered carbon is surprising, particularly since the same paper reported an anomalously low value of 6.8 μF/cm$^2$ for GC. The smooth surface of PPF must be at least partly responsible for its low capacitance, since its roughness factor (ratio of microscopic to geometric area) is lower than that of polished GC. The SEM, AFM, and Raman results indicate a very smooth surface with no features observable by light microscopy and an apparent AFM roughness of <10 Å. An additional factor that may contribute to low capacitance is the electronic structure of PPF compared to GC, a property that is strongly dependent on thermal history. There is no direct evidence for an electronic contribution at present, but it remains a possibility.

**Table VII. Representative characteristics of GC and pyrolyzed carbon films.**

| Fabrication method | Resistivity (mΩ cm) | Capacitance (μF cm$^2$) | $k^0$ [a] $Fe(CN)_6^{3-/4-}$ | Reference |
|---|---|---|---|---|
| GC-20, Tokai, polished | 4 | 33 | 0.06-0.15 | 7, 28, 29 |
| GC-20, forming gas, 1000°C | 4 | 22 | 0.044 | Current work |
| Poly(furfuryl alcohol) pyrolysis, 1100°C | 10 | | | 22 |
| Polyacrylonitrile pyrolysis, 1020°C | 2 | | | 20 |
| Methane pyrolysis, 1100°C | | 20 | 0.004[b] | 12 |
| Natural gas pyrolysis, 1000°C, on Macor | | >100 | 0.004-0.015 | 9 |
| Methane pyrolysis | | 32 | 0.009 | 8 |
| Organic film pyrolysis, 1000°C | 4 | | | 15 |
| Sputtered carbon | 35 | 7.5 | 0.024-0.042[c] | 16 |
| PPF forming gas, 1100°C | 5.1 | 8.1 | 0.015[d] | Current work |
| | | | 0.042[e] | |

[a] In 1 M KCl unless indicated otherwise.
[b] Calculated from voltammetric data in Ref. 12.
[c] In 0.5 M $H_2SO_4$.
[d] From observed $\Delta E_p$ at 2 V/s.
[e] Same as d, corrected for film resistance.

S0013-4651(99)02-055-8 CCC: $7.00 

The very smooth surface of PPF, with no observable porosity, implies a formation mechanism similar to liquid curing. Microscopic bubbles formed during outgassing are apparently filled by the hot film during pyrolysis. However, macroscopic flow was not observed, and the ~88 μm gap apparent in Fig. 6 was maintained during pyrolysis. Shrinkage occurred predominantly in the vertical direction, and the final surface was free of observable porosity or pinholes. Liquid curing is not the only possibility for a formation mechanism, but it is consistent with a smooth surface of the cured films.

The curing atmosphere was studied in detail because of its likely effect on the surface O/C ratio. The high vacuum ($10^{-7}$ Torr) generally yielded the lowest O/C ratio up to 1000°C, but was not available at 1100°C with the apparatus used here. Forming gas is significantly simpler to implement than ultrahigh vacuum, requiring only a furnace and no pumps. The 5% hydrogen in forming gas should counter the trace oxygen present in most pyrolysis atmospheres, permitting the formation of very low O/C surfaces. In addition, the PPF surfaces showed low rates of increase in O/C compared to heat-treated GC, when monitored over several days of air exposure. We can speculate that this lower reactivity is due to a lower density of unsatisfied valences on PPF compared to GC, and lower reactivity with oxygen as a result. It is possible that pyrolysis in forming gas leads to a hydrogen-terminated surface, similar to that of hydrogen-terminated glassy carbon.[32] The O/C ratio for hydrogen-terminated GC has been shown to increase very slowly upon air exposure.[32]

In closing, we can consider pyrolyzed photoresist pyrolysis to be another of many carbon materials suitable for electrochemistry. In this regard, it has the attractive properties of low background current, a smooth surface, and a low O/C ratio compared to GC. It exhibits electron-transfer kinetics for $Fe(CN)_6^{3-/4-}$ and $Ru(NH_3)_6^{3+/2+}$ comparable to those of other carbon films. In addition to these attractive electrochemical properties is the ability to use photolithography to make electrode patterns, demonstrated by Fig. 6. Analytical devices based on pyrolysis of lithographic patterns may be mass produced, in principle, and may be the basis of high volume electrochemical sensors. The stability, adsorption properties, and electron-transfer kinetics of pyrolyzed photoresist are currently under investigation for a much wider range of redox reactions and potential electroanalytical applications based on carbon-MEMS.

## Acknowledgments

This work was supported in part by the National Science Foundation (N.S.F) Division of Analytical and Surface Chemistry. The authors acknowledge useful conversations with Dr. Kim Kinoshita, Lawrence Berkley National Laboratory, Berkeley, California.

*Ohio State University assisted in meeting the publication costs of this article.*

## References

1. M. Madou, *Fundamentals of Microfabrication,* CRC Press, New York (1997).
2. J. Kim, X. Song, K. Kinoshita, M. Madou, and R. White, *J. Electrochem. Soc.*, **145,** 2315 (1998).
3. R. L. McCreery, K. K. Cline, C. A. McDermott, and M. T. McDermott, *Colloids Surf.*, **93,** 211 (1994).
4. K. Kinoshita, *Carbon: Electrochemical and Physicochemical Properties*, John Wiley & Sons, New York (1988).
5. R. L. McCreery, in *Electroanalytical Chemistry,* Vol. 17, A. J. Bard, Editor, p. 221, Marcel Dekker, New York (1991).
6. R. L. McCreery, in *Laboratory Techniques in Electroanalytical Chemistry,* 2nd ed., P. T. Kissinger and W. R. Heineman, Editors, Chap. 10, Marcel Dekker, New York (1996).
7. R. L. McCreery, in *Interfacial Electrochemistry,* A. Wieckowski, Editor, Chap. 35, Dekker, New York (1999).
8. A. L. Beilby and A. Carlsson, *J. Electroanal. Chem.*, **248,** 283 (1988).
9. C. F. McFadden, L. L. Russell, P. R. Melaragno, and J. A. Davis, *Anal. Chem.*, **62,** 742 (1990).
10. J. K. Clark, W. A. Schilling, C. A. Wijayawardhana, and P. R. Melaragno, *Anal. Chem.*, **66,** 3528 (1994).
11. R. A. Saraceno, C. E. Engstrom, M. Rose, and A. G. Ewing, *Anal. Chem.*, **61,** 560 (1989).
12. K. Lundstrom, *Anal. Chim. Acta*, **146,** 97 (1983).
13. K. Lundstrom, *Anal. Chim. Acta*, **146,** 109 (1983).
14. A. Rojo, A. Rosenstratten, and D. Anjo, *Anal.Chem.*, **58,** 2988 (1986).
15. O. Niwa and H. Tabel, *Anal. Chem.*, **66,** 285 (1994).
16. R. Schlesinger, M. Bruns, and H.-J. Ache, *J. Electrochem. Soc.*, **144,** 6 (1997).
17. A. M. Lyons, L. P. Hale, and C. W. Wilkins, *J. Vac. Sci. Technol., B,* **3,** 447 (1985).
18. A. M. Lyons, *J. Non-Cryst. Solids*, **70,** 99 (1985).
19. J. Wang, Q. Chen, C. L. Renschler, and C. White, *Anal. Chem.*, **66,** 1988 (1994).
20. C. L. Renschler, A. P. Sylwester, and L. V. Salgado, *J. Mater. Res.*, **4,** 452 (1989).
21. O. J. A. Schueller, S. T. Brittain, C. Marzolin, and G. M. Whitesides, *Chem. Mater.*, **9,** 1399 (1997).
22. O. J. A. Schueller, S. T. Brittain, and G. M. Whitesides, *Sens. Actuators,* **A72,** 125 (1999).
23. O. J. A. Schueller, S. T. Brittain, and G. M. Whitesides, *Adv. Mater.*, **9,** 477 (1997).
24. R. Lum, C. Wilkins, M. Robbins, A. Lyons, and R. Jones, *Carbon,* **21,** 111 (1983).
25. M. T. McDermott, C. A. McDermott, and R. L. McCreery, *Anal. Chem.*, **65,** 937 (1993).
26. Y. Wang, D. Alsmeyer, and R. L. McCreery, *Chem. Mater.*, **2,** 557 (1990).
27. M. S. Dresselhaus, G. Dresselhaus, K. Sugihara, I. L. Spain, and M. A. Goldberg, *Graphite Fibers and Filaments*, 98, Springer-Verlag, New York (1988).
28. P. Chen and R. L. McCreery, *Anal. Chem.*, **68,** 3958 (1996).
29. I. F. Hu, D. H. Karweik, and T. Kuwana, *J. Electroanal. Chem.*, **188,** 59 (1985).
30. S. Ranganathan, T.-C. Kuo, and R. L. McCreery, *Anal. Chem.*, **71**, 3574 (1999).
31. W. M. Moreau, in *Semiconductor Lithography,* Plenum Press, New York (1988).
32. T.-C. Kuo and R. L. McCreery, *Anal. Chem.*, **71,** 1553 (1999).